

SEISMIC PERFORMANCE OF IMPROVED PILE-TO-WHARF DECK CONNECTIONS

Dawn E. Lehman, Associate Professor, University of Washington

Charles Roeder, Professor, University of Washington

Stuart J. Stringer, Berger/ABAM

Amanda Jellin, HDR Engineering

ABSTRACT

Pile-supported marginal wharves are critical components of the nations infrastructure, and post-earthquake functionality is essential. Previous earthquakes demonstrate that pile-wharf connections are vulnerable to earthquake damage. Current connection design uses headed dowel bars to connect vertical, precast concrete piles to the deck. Although prior research studies indicate these dowel connections have adequate resistance, the connections sustained damage in the pile and deck, even at moderate deformations, which results in strength deterioration. Even moderate damage requires post-earthquake repair, which is difficult to access and economically disruptive. A research program was undertaken to reduce seismic connection damage through the development of a new pile-wharf connection. To mitigate the pile and deck damage, several structural concepts were experimentally evaluated including (1) intentional debonding of the dowel bars, (2) employing a bearing pad between the head of the pile and the deck, and (3) adding a flexible joint around the embedded portion of the pile. A prototype connection was developed and further studied experimentally to investigate the impact of axial load, bearing-pad material and bearing-pad configuration. The proposed connection reduces damage and strength deterioration relative to current connection, including delaying pile and deck spalling well beyond the expected seismic deformation demand level. The experimental observations and measures were used to develop performance-based design expressions and a design procedure for this new connection.

Keywords: precast piles, connections, seismic design, marginal wharves, performance based design

INTRODUCTION

Ports are a vital link in the transportation of goods worldwide, with more than a trillion dollars of goods flowing through US shipping terminals every year (Port of Seattle, 2009). Economies worldwide rely heavily on ports, and it is estimated that \$1,000 is brought into the local economy from each shipping container. Many ports are located in high seismic regions and are susceptible to strong ground motions, resulting in the potential for devastating physical and economic damage. In addition, most ports are built on poor soils that are susceptible to liquefaction, lateral spreading, and differential settlements, which compound the likelihood of earthquake damage.

Economically, ports damaged by earthquakes require repair. Equally or more important, ports suffer loss of income and reduced activity due to repair downtime. The loss in income can be long-term or permanent, since tenants move to other regional ports while the damaged port is repaired, and may not return after repairs are completed. An example of this was found after the 1995 Hanshin earthquake. Prior to the earthquake, the Port of Kobe was ranked as the 6th busiest port for container shipping in the world. In 1997, shortly after the earthquake, the port had slipped to 17th, and by 2005 it had dropped to 39th (Chang 2000).

Because of the short-term and long-term vulnerability, ports must be designed to not only withstand strong ground motions, but they should sustain minimal seismic damage. Most marginal wharves are partially or fully supported by plumb precast, prestressed concrete piling, as depicted in Fig. 1a. Vertical pile-supported wharf structures are designed to act as a ductile moment frame with plastic hinge formation at the connection to the wharf deck; a second hinge may form below the surface of the soil. As a result of the framing action, these connections experience significant moment and rotation demands, and they are vital to the overall performance of the system. These connections are typically variations of the embedded dowel connection, as shown in Fig. 1b., or the extended pile connection, as shown in Fig. 1c. (Extended pile connections are only required when the pile is driven below the deck level to achieve the required bearing capacity and are not preferred.) Prior research suggests that these connections are vulnerable to seismic damage (Roeder et al. 2005).

Figure 1a shows that the unsupported pile lengths within a marginal wharf vary greatly, and the shear force, bending moment, and deformation demands on each connection in the structure are functions of this length. The waterside piles can have upwards of 15 m (50 feet) of unsupported length while the landside piles may be 3 m (10 feet) or less. Typically the wharf deck is heavily reinforced and stiff, causing the deck to displace rigidly under seismic lateral loading.

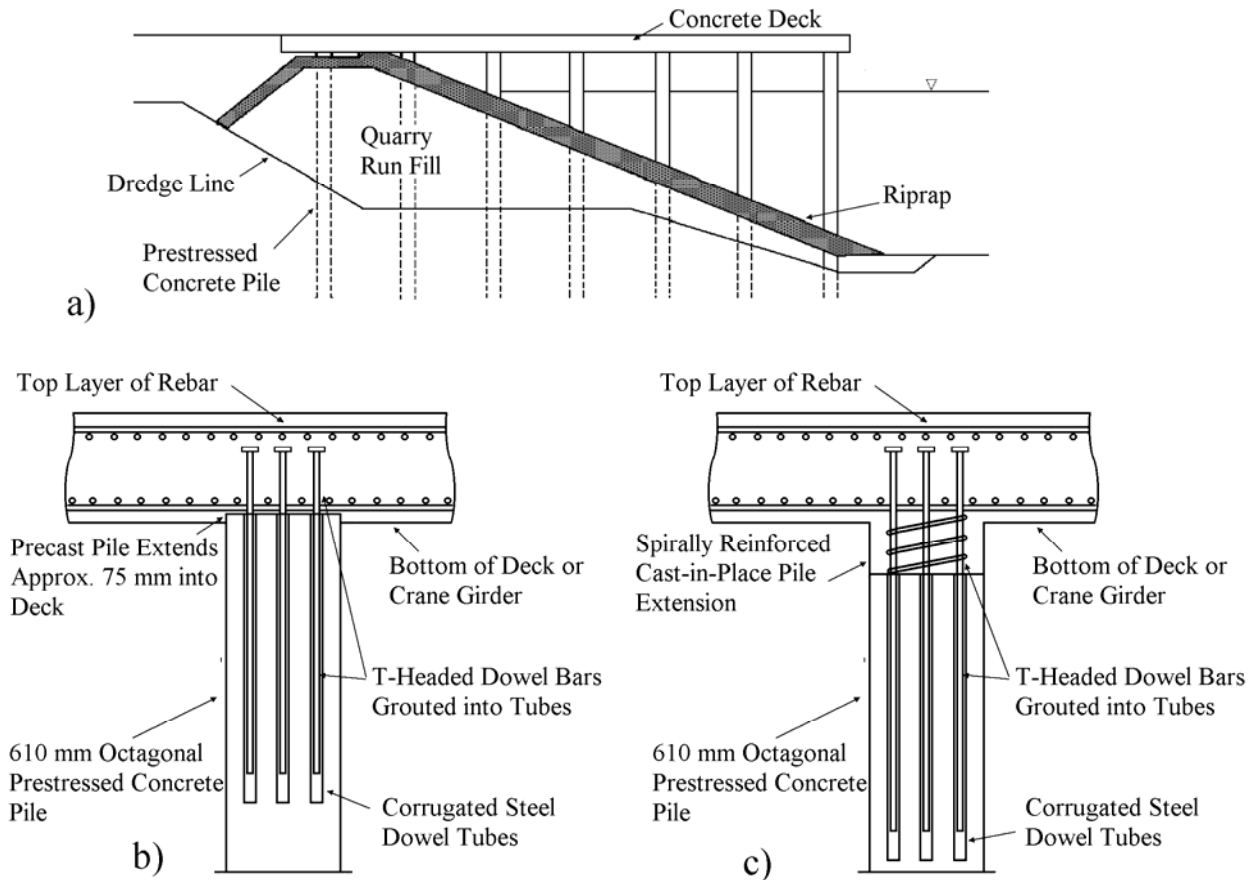


Figure 1. Typical Current Marginal Wharf Practice, a) Wharf Cross Section, b) Embedded Dowel Connection, and c) Extended Pile Connection

PREVIOUS RESEARCH ON DOWEL CONNECTIONS

A number of past studies have examined the seismic performance of embedded dowel connections and extended pile connections (Joen and Park 1994, Sliva et al. 1997, Silva 1998, Sritharan and Priestley 1998, Graff 2001, Soderstrom 2001, and Roeder et al. 2005). The details of the test specimens vary widely, but consistent observations can be made from those test results.

Figure 2 demonstrates some of these observations through consideration of the lateral resistance-deflection and moment-rotation behavior of three test specimens. Figure 2a shows the behavior for an extended pile connection without axial load, while Figs. 2b and 2c show the behavior for embedded dowel connections with precast concrete piles without and with axial, respectively. The axial load for the connection of Fig. 2c was approximately 10% of the axial load ($0.1f_c A_g$) capacity of the prestressed pile, which is within the range of the axial loads expected in practice.

Figs. 2a and 2b show the fundamental differences in the behavior of the extended-pile connection and the embedded-dowel connection. The extended-pile connection behaves largely as cast-in-place reinforced concrete connection and limits deterioration and loss of resistance to larger drifts. The precast-pile connection without an axial load has more deterioration in resistance and moment capacity but similar maximum resistance to an identical extended pile connection.

Precast piles deteriorate at lower deformations and more severely than a cast-in-place column-deck connection, because the flexural deformations are limited in the pile, which largely act as a rigid body and rock with connection rotation. The connection must sustain the cyclic deformations demands. The rocking action causes large edge stresses on the pile and wrenching action of the end of the pile that is embedded into the deck. This leads to early spalling of the pile and deck, such as shown in Fig. 3c. Typically, the cover on the pile is large (more than 76 mm), to prevent corrosion of the prestressing strands and loss of this cover results in a more significant decrease in the bending resistance than a typical reinforced concrete column. This loss of concrete cover results in loss of resistance with increasing deformation, as shown in Figs. 2b and 2c. Extended pile connections are used only in special cases where the pile is driven below the bottom of the soffit of the wharf deck. As a result, dowel connections with precast piles are most common and do not meet the performance expectations.

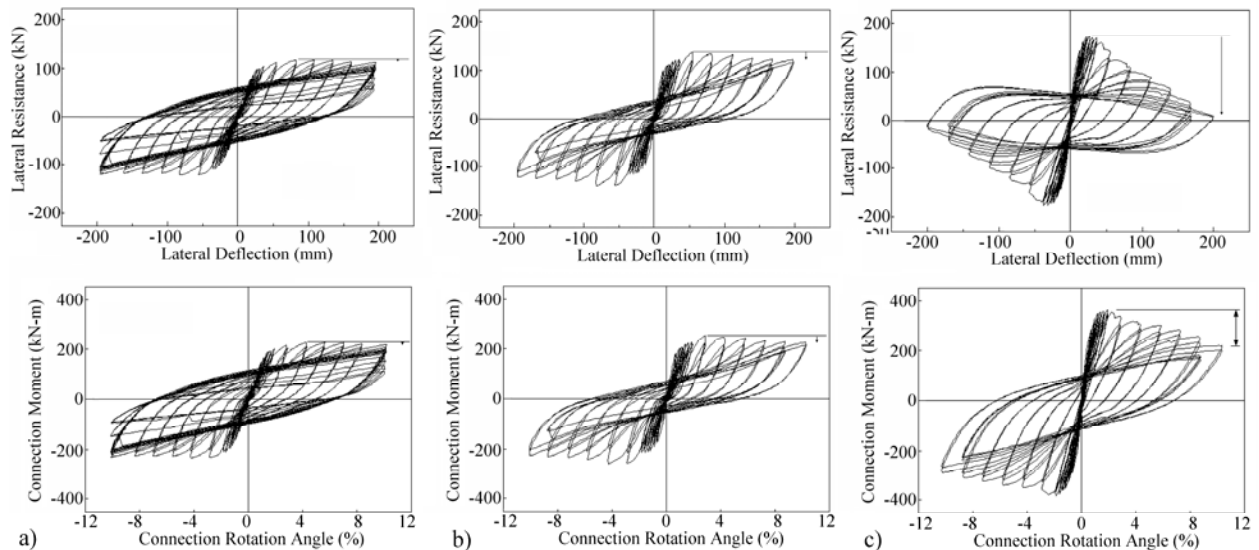


Figure 2. Typical connection force-deflection and moment-rotation results, a) Extended pile with no axial load, b) Precast pile with no axial load, and c) Precast pile with 10% axial load.

The axial stress demand is important. In a marginal wharf application, the piles support compressive load due to the heavy deck system. The addition of compressive load to the pile significantly changes the connection response, as seen by comparing Figs. 2b and 2c. It is of note that the pile is prestressed, which results in large compressive stresses. The addition of an axial load of only 10% of the gross axial capacity, as was used for the specimen that

resulted in the measured behavior in Fig. 2c, significantly changes the response. The axial load significantly increases the moment capacity and maximum lateral resistance of the connection, but it also dramatically increases the rate of deterioration in resistance. Part of the lost lateral resistance can be attributed to P- Δ effects at large deflections (compare the deformation in the force-deflection and moment-rotation plots of Fig. 2c). These P- Δ moments reduce the lateral resistance because a portion of the moment capacity is consumed by P- Δ effects.

The deterioration noted with the moment-rotation curves is a true measure of damage to the pile and its connection. At large rotations, the compressive force at the edge of the pile, associated with the bending moment and further increased by the axial load, results in large compressive stresses (Roeder et al. 2005). Hence, with an increase in axial force, spalling occurs at smaller deformations (Figs. 3a and 3b) and is more severe resulting in larger deterioration (Figs. 2b and 2c)

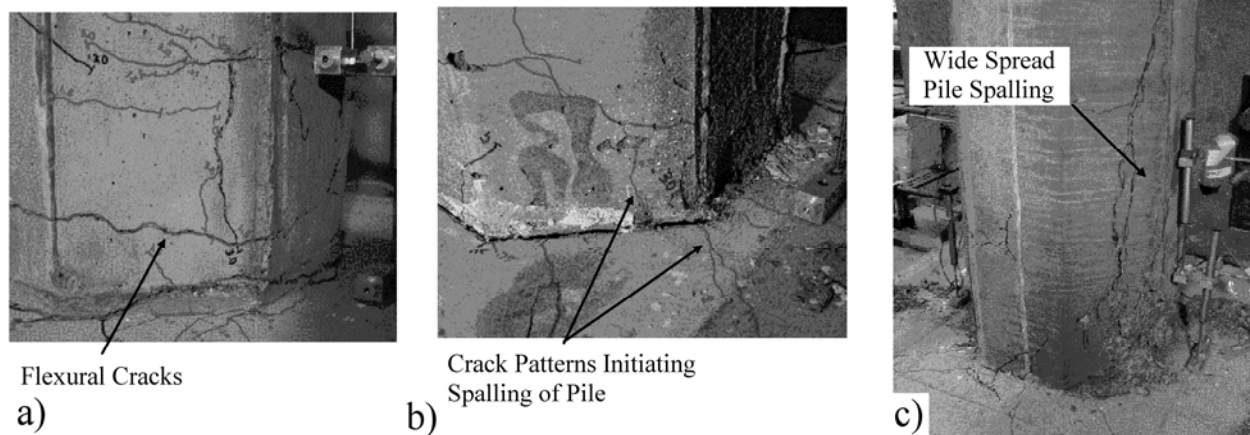


Figure 3. Photos of pile connections; a) Extended pile with no axial load, b) Precast pile with no axial load, and c) Precast pile with 10% axial load.

Figure 3 shows damage of the three connections at the same connection rotation level of 0.03 radians. The actual displacement of the pile depends on its effective length. For a short pile at the end of the wharf, the displacement associated with this level of rotation is relatively small since the effective pile length is small. The extended pile connection (Fig. 3a) is largely intact with flexural cracking. The precast pile with a dowel connection and no axial load (shown in Fig. 3b) is still intact, but the crack pattern suggests that spalling will initiate at slightly larger deformations.

The precast pile with a dowel connection and axial load, shown in Fig. 2c and 3c, sustains significant spalling damage. Other specimens exhibited this level of spalling, but at significantly higher wharf displacements and connection deformations. Pile and deck spalling have structural implications beyond seismic resistance, since they cause loss of prestressing force and expose the reinforcing steel to the harsh marine environment. Hence, repairs are required for these connections even after modest earthquakes. However, the spalling and its

correlation to the deterioration in resistance suggest that the performance of the connections may be significantly improved at all performance levels if spalling is delayed.

CHARACTERISTICS OF A DAMAGE-RESISTANT PILE-WHARF CONNECTION

A research program was undertaken to improve the seismic performance of pile-to-wharf connections. The study examined the results of prior research, evaluated recent wharf and pile connection designs, and, in consultation with practicing engineers in this field, developed improved connection designs. Experiments were conducted to investigate the connection designs. Several options were proposed for experimental evaluation, including:

- Partial debonding of the dowel bars into the wharf deck and the pile itself. Debonding reduces the maximum strain demand in the steel. For a given level of strain, a debonded bar has a larger axial deformation than a bonded bar, a direct result of the strain gradient (uniform vs. non-uniform). This delays dowel bar fracture and increases the rotation for a given level of strain demand (Stanton et al. 1997). This technique has been used successfully in precast, prestressed moment frames for buildings. A second feature of debonding the dowel bars is that it alleviates bond stress transfer in that region, which can damage the deck concrete.
- Addition of a flexible material between the pile and deck to sustain the rotation demands and reduce damage. As demonstrated by Figure 3, rocking of the pile under cyclic loading results in edge loading of the pile and contributes to premature concrete damage. To reduce the damage, the edge loading needs to be distributed to a larger area of the pile cross section to reduce the compressive stress demands. Here, a bearing pad manufactured of a material strong enough to sustain the compressive stress demands but flexible enough to sustain the rotation demands was used.
- Flexible joint sealant wrap around the embedded perimeter of the pile. There was discussion with the engineers to modify the 75 to 100 mm (3 to 4 inch) embedment of the pile into the wharf deck, by either increasing the embedment depth or eliminating it. This short embedment is approximately equal to the cover depth, and results in high shear stress demands on unreinforced concrete which in turn results in significant concrete damage. It was postulated the either a much larger or elimination of the embedment depth would reduce the spalling of the deck at larger rotations. However, the practicing engineers deemed neither option acceptable. The concerns were that eliminating the embedment depth would (1) result in intrusion of salt water into the connection and (2) decrease the shear resistance. As an alternative, a gap was placed between the pile and deck and filled with a flexible material, to reduce the shear stress demands. This material seals the joint to prevent intrusion of salt water into the connection.

EXPERIMENTAL PROGRAM

An experimental program was initiated at the University of Washington to investigate pile-wharf connections with these damage-mitigating characteristics. Eight full-scale precast

concrete pile-wharf deck connections were tested (Jellin 2008, Stringer 2010) and included one or more of these aspects of the connections, as well as the applied axial load and the bearing pad configuration and material. The eight test specimens had the same piles and deck reinforcing and configuration, which are illustrated in Figs. 4 and 5. These aspects of the specimen design were determined from an infrastructure review of 14 marginal wharf structures from the Port of Los Angeles, the Port of Oakland, and the Port of Seattle.

The specimens had a 610-mm prestressed concrete pile and utilized an embedded T-headed dowel bar connection. The pile had twenty-two 12.7mm diameter low relaxation strands with strengths of 1,860 MPa. The strands were pretensioned to 138 kN, resulting in a service level prestress of approximately 9.7 MPa after accounting for relaxation stress losses. The spiral reinforcement was W11 (9.5mm diameter) smooth wire, and the pitch varied along the length of the pile from 25mm at the ends to 76mm in the middle, as shown in Fig. 4. All of the piles were donated by Concrete Technology Corporation.

Compressive strength data up to the 28-day strength was provided but test cylinders were not available for the day of test strength. The pile concrete was a 9.5 mm (5/8") max aggregate 55.1 MPa (8,000 psi) mix with a 76-229 mm (3" – 9") slump. The piles used for the test were cast from one of three different batches, which had 28-day strengths of 66.7 MPa (9680 psi), 73.4 MPa (10,648 psi) and 58.0 MPa (8410 psi). Due to incomplete documentation, determining which pile came from which batch was not possible.

The piles were embedded 76mm into a cast-in-place reinforced concrete section representing a segment of the deck. The connection was made using eight ASTM A706 (482 MPa yield stress) No. 10 T-headed dowel bars, which were embedded 508mm into the deck. The dowels were 1.93m long and were grouted 1.5m into corrugated ducts in the pile using high strength, non-shrink grout. The grout achieved 34.5 MPa and 69 MPa compressive strengths in 24 hours and 28 days, respectively.

The pile length was 2.62m from the soffit of the deck to the horizontal loading point, and this length was chosen to be representative of short pile length in typical wharf structures based on prior analyses (Yoo 2001). The deck dimensions (see Fig. 5) were maximized to ensure simulation of force transfer without interference from the test setup, but constrained to fit into the test rig. The deck reinforcement is shown in Fig. 5 and simulates reinforcement layouts typically used in the prototype marginal wharves.

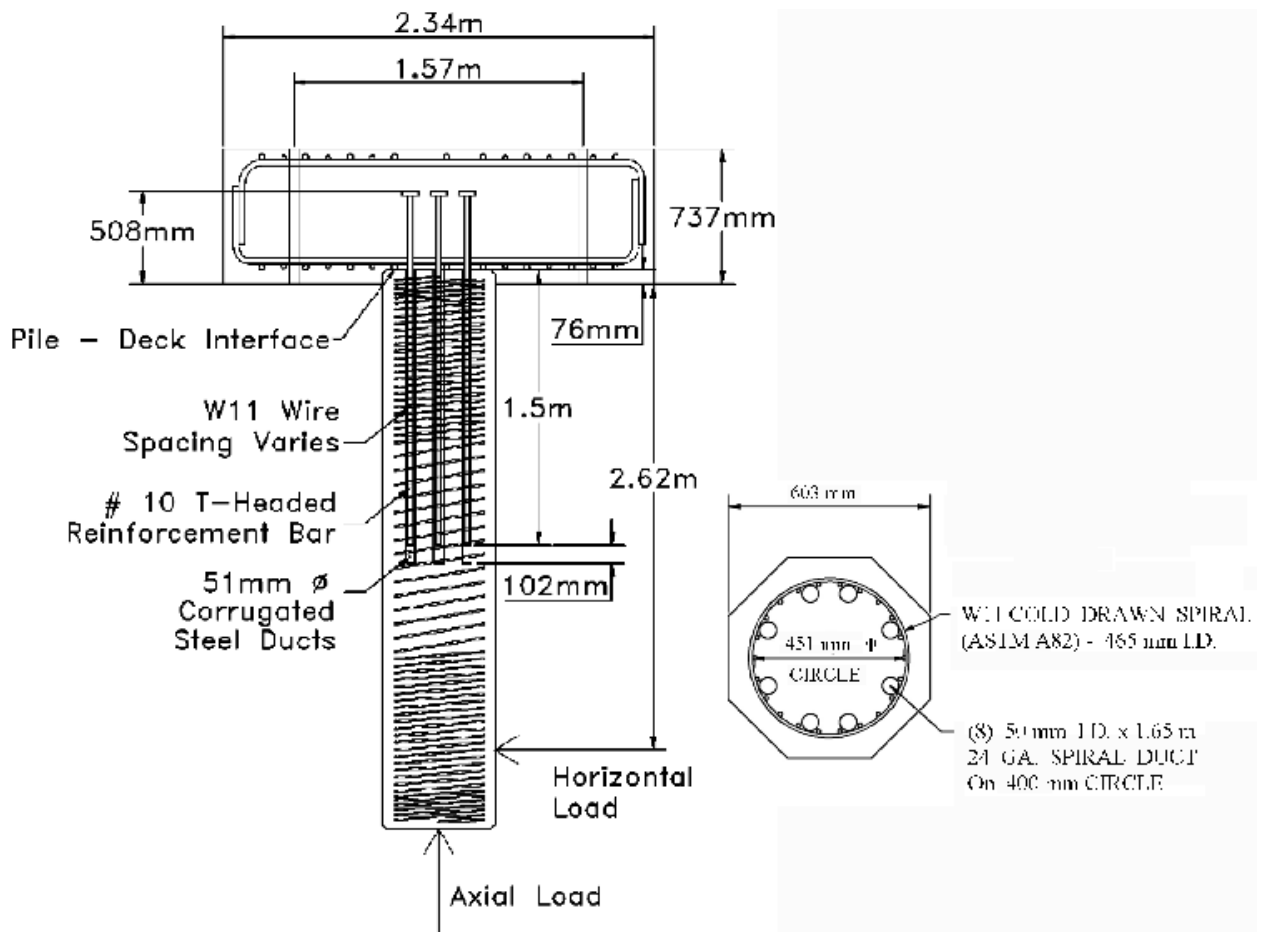


Figure 4. Overall specimen dimensions and reinforcing steel

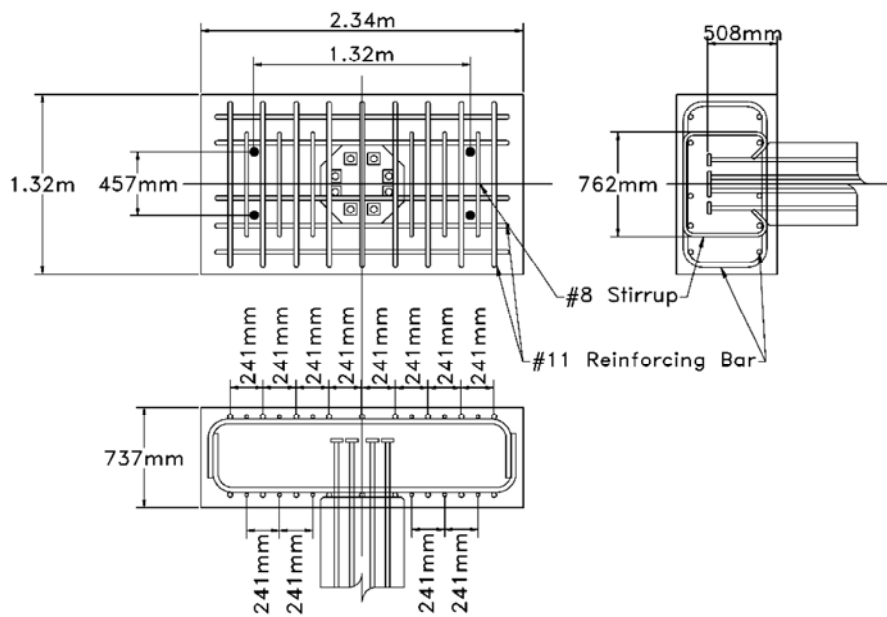


Figure 5. Deck reinforcement (all specimens)

The specimens are identified as Specimens 9 through 16 (numbered to be consecutive with the specimens studied by Graff 2001 and Sodersom 2001) and are presented in Table 1 and Fig. 6. The specimens studied the connection modifications, axial load, and bearing pad characteristics. The primary study parameter for each specimen is shown in bold font in the table. A brief description of each specimen follows.

- Specimen 9 used the embedded dowel bar connection commonly used in current design and serves as the reference specimen.
- The dowel bars in Specimen 10 were intentionally debonded into the connection and into the deck, 190 mm for each. All other aspects of the connection were the same as Specimen 9.
- The connection of Specimen 11 included the debonded region and the addition of a cotton-duck bearing pad (CDP) between the pile and deck interface. CDP have high compressive strength and can accommodate large rotations (Lehman et al. 2005). All bearing pads had an octagonal shape with 610 mm outside dimensions to cover the entire head of the pile.
- Specimen 12 was identical to Specimen 11 (with a debonded region and a CDP) with the addition of a soft foam wrap that was added around the perimeter of the length of the pile embedded into the deck.
- Specimen 13 was nominally identical to Specimen 12 to investigate use of different materials in the gap between the pile and the deck. Specimen 13 used a CERAMAR flexible expansion material (CFEM) for this gap (Meadows 2001).
- Specimen 14 was nominally identical to Specimen 13 but subjected to twice the axial load.
- Specimens 15 and 16 explored the effects of using different bearing pads. Specimen 15 had an annular 19mm CDP to improve constructability. Specimen 16 had a 13mm random oriented fiber bearing pad (ROFP). These annular rings pads had 457mm diameter center hole that cleared the dowels and ducts of the pile.

TABLE 1. DETAILS OF TEST SPECIMENS (STUDY PARAMETER IN BOLD)

Specimen	Axial Load (kN)	Debonded Length (mm)	Interface Bearing Pad	Pile Isolation	Yield Stress of Dowel (MPa)
9	2,000	None	None	None	495
10	2,000	381	None	None	495
11	2,000	381	19mm Full CDP	None	480
12	2,000	381	19mm Full CDP	19mm foam	480
13	2,000	381	19mm Full CDP	19mm CFEM	445

14	4,000	381	19mm Full CDP	19mm CFEM	445
15	2,000	381	19mm Annular CDP	19mm CFEM	445
16	2,000	381	13mm Annular ROFP	19mm CFEM	445

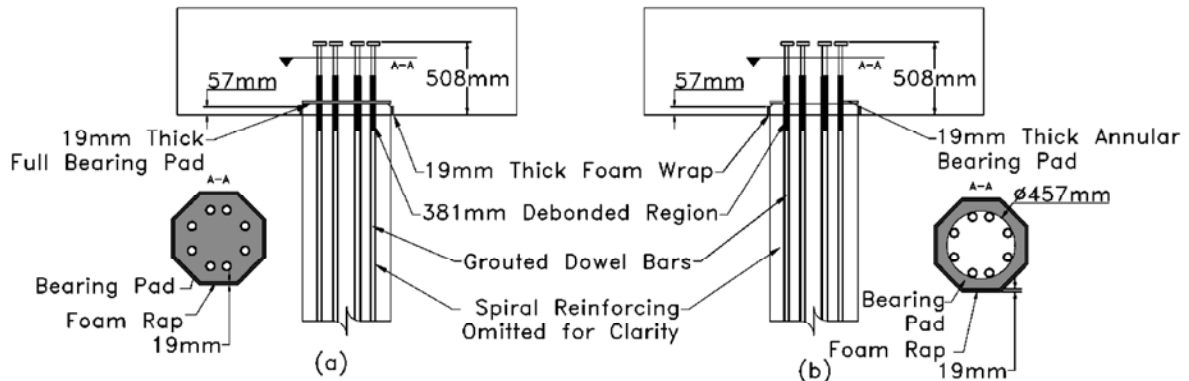


Figure 6. Test specimen details (deck and pile spiral reinforcement not shown)

TEST SETUP AND PROCEDURE

The specimens were constructed to simulate the field orientation (deck cast above the pile), however were tested in an inverted position to fit within the constraints of the test setup and laboratory. A self-equilibrating test rig, shown in Fig. 7, was used. The deck portion of the specimen was post-tensioned to a reaction block at the base of the test frame using four 32mm, 1,034 MPa high strength threaded rods, post tensioned to 556 kN.

The vertical axial load was applied by a 10.6 mN Baldwin universal testing machine (UTM). An assembly was constructed to ensure the axial load imparted minimal horizontal force on the loading head of the UTM. A recessed, dimpled, and lubricated polytetrafluoroethylene (PTFE) sliding surface with a mirror finished stainless steel plate mating was set inside a C15x15 section, which was attached to the UTM loading head. A spherical bearing was placed below the PTFE sliding surface to accommodate end rotation of the pile tip.

The horizontal cyclic load was applied using a 977-kN, 508mm stroke MTS actuator, which was attached to and reacted against the test frame. The actuator was connected to the pile using, four 22mm B7 steel rods and two 25.4mm thick steel plates placed on either side of the pile. A 3.2mm elastomeric pad was placed between the steel plates at the end of the actuator and the face of the pile to evenly distribute the bearing stresses.

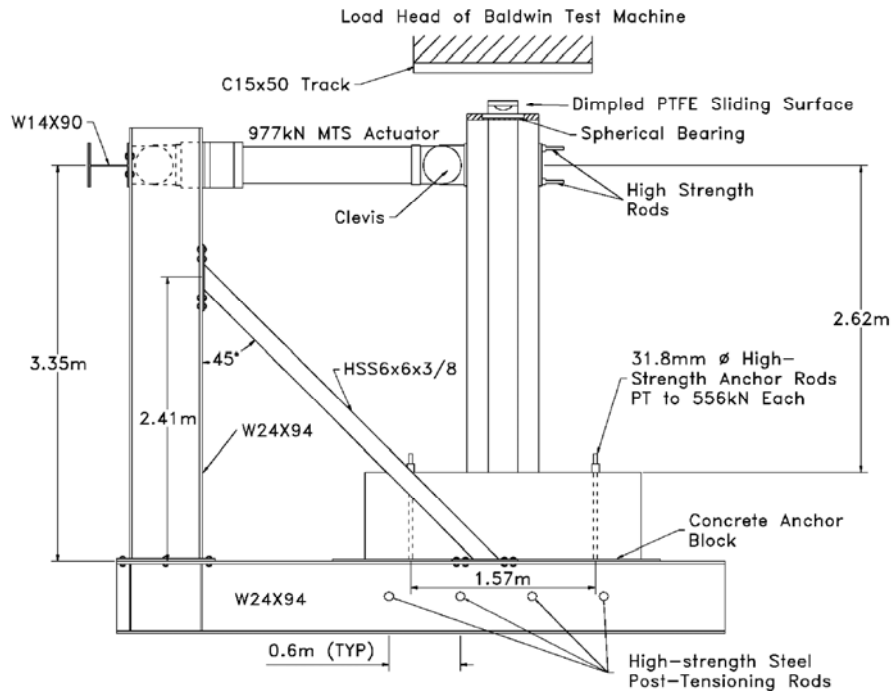


Figure 7. Test rig

The specimens were subjected to a constant vertical load. The cyclic lateral loads were applied under displacement control with increasing amplitude deformation cycles with a test protocol based upon the ATC 24 procedure (ATC 1992).

Figure 8 shows the external instruments used to monitor the specimen. String pots were used to monitor the horizontal movement at several locations along the pile length (P9-P11). Vertical potentiometers were used to monitor segment rotations, from which average curvatures could be calculated (P14-P21). The bottommost vertical potentiometers monitored connection rotation (P5-P6). Other potentiometers monitored specimen slip, overturning, and movement of the setup. Finally a series of inclinometers were placed on either face of the specimen to monitor rotation; the inclinometers are shown at the lower end of the pile in the figure. Additional details of the test specimens, setup and instrumentation can be found in Stringer (2010).

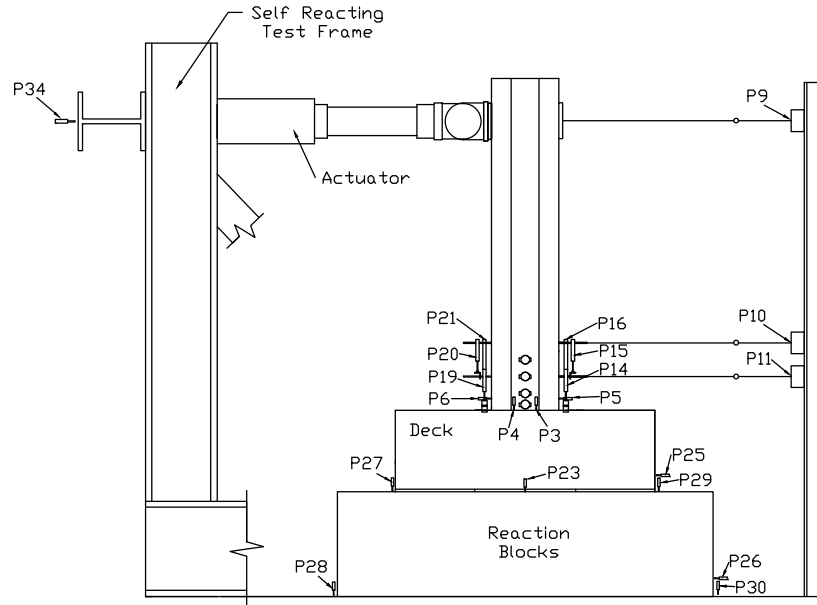


Figure 8. Overview of Instrumentation Layout

EXPERIMENTAL RESULTS

Assessment of the specimen performance was made through consideration of the damage sustained through loading and the measured global response. The moment-rotation response for six specimens is provided in Figure 9. (Note that maximum moment-rotation response is shown because the force-drift response curves include degradation resulting from P-delta effects. The moment-rotation curves show the actual specimen response.) Key characteristics that are important to understanding the specimen response and performance are provided in Figure 10.

Specimen 9 was the reference specimen and simulated current practice; it provides a baseline comparison for the other specimens. As shown in Figure 9, the connection reached its peak moment resistance at a connection rotation of 1.4% and deterioration of resistance initiated shortly thereafter. At the connection rotation of 8%, four dowel bars had fractured and the moment resistance dropped to 47% of the maximum. At this deformation, the lateral resistance was essentially zero because of the deterioration and P- Δ moments. Figure 10 shows the observed response at approximately 2.5%, 4% and 8.4% rotation angle, which are approximately the damage states corresponding to initial spalling, substantial spalling (includes complete spalling of the cover and up damage to the core), and bar fracture.

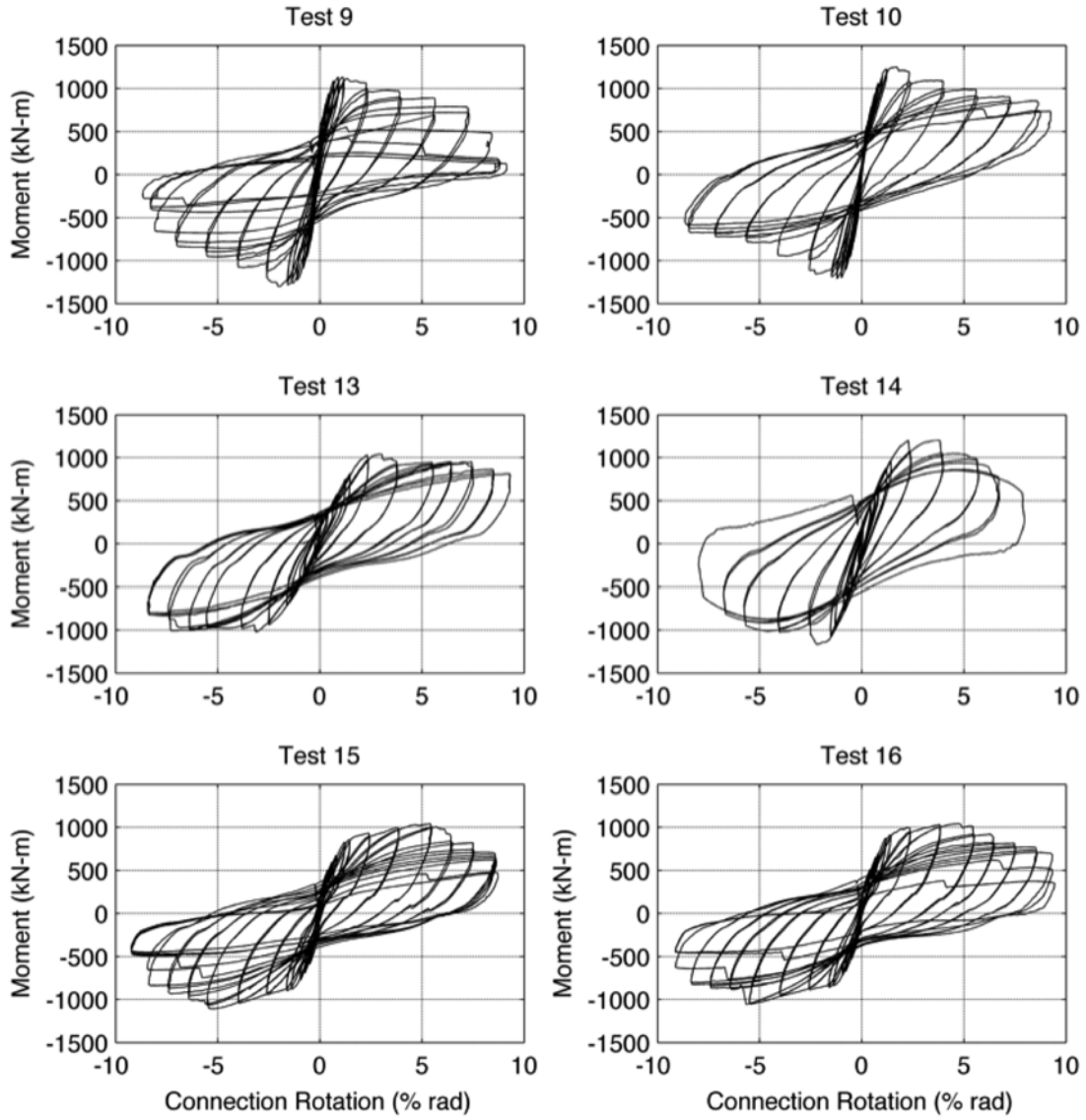


Figure 9. Moment-rotation Hysteretic Response for Six Key Specimens

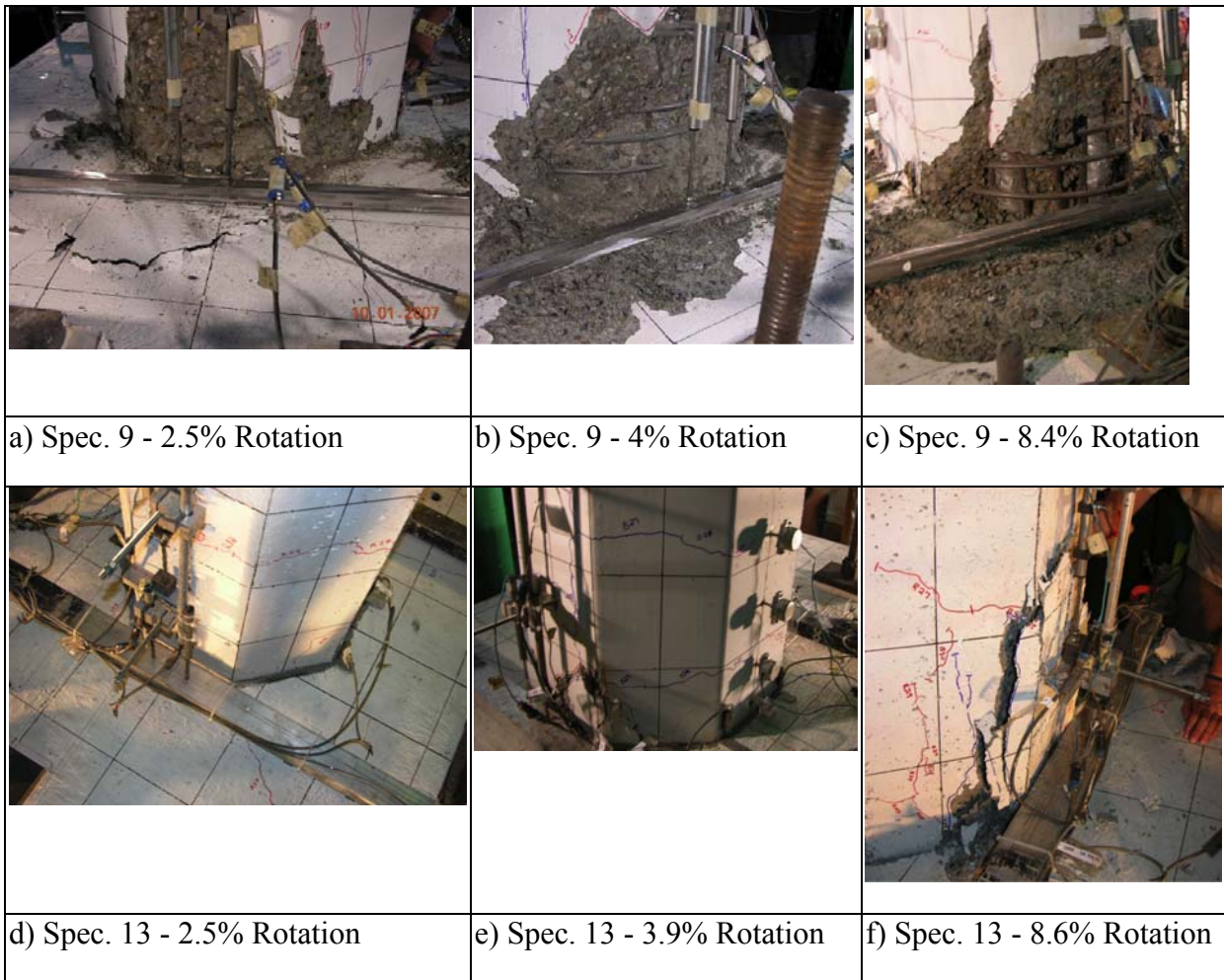


Figure 10. Comparisons of Connection Performance

Specimens 10-13 investigated fundamental improvements to the connection. Specimen 10 had debonded dowel bars and exhibited similar moment and shear capacities but with reduced deterioration in resistance than Specimen 9. The debonded dowel bar steel caused initial pile cover spalling to occur at a slightly lower rotation, but delayed both substantial spalling and dowel bar fracture. The hysteretic loops of Specimen 10 show significantly less degradation in resistance than Specimen 9 between 8% and 9% connection rotation despite experiencing dowel bar fracture.

Figures 9 and 10 and Table 2 show that Specimen 13 exhibited markedly different behavior than Specimens 9 and 10. Specimen 13 included debonded dowel bars as well, however it was the addition of a 19mm thick 610mm diameter octagonal CDP, and a 19mm thick CFEM wrap around the perimeter of the embedded pile segment that greatly reduced the damage at moderate to large levels of drift. The behavior of Specimen 13 is much improved in comparison with Specimens 9 and 10 as shown by comparisons in Fig. 10, since it provided considerable delay in initial and substantial spalling, which occurred at 3.8% and 8.4%

connection rotation, respectively. No dowel bars fractured during this test despite deformation cycles to 8.9% connection rotation. By 8% connection rotation the moment resistance had only reduced by 19% of the peak resistance, which is considerably less than either Specimens 9 or 10. However, despite these significant improvements in performance the addition of the full bearing pad reduced the elastic stiffness of the connection by nearly 50% compared to Specimens 9 and 10.

Table 2. Performance Characteristics of Six Key Specimens

Specimen	Peak Shear	Moment Capacity	Normalized Moment Capacity	Elastic Rotational Stiffness 1% Rot.	Initial Spalling	Substantial Spalling	Bar Fracture	Decrease in Moment 8% Rot.
					Rotation (percent)			
9	436 kN	1,216 kN-m	1.07	1,330 kN-m/% rad	1.42%	3.98%	8.21%	53%
10	440 kN	1,228 kN-m	1.08	1,330 kN-m/% rad	1.19%	5.64%	8.52%	40%
13	334 kN	1,029 kN-m	0.99	530 kN-m/% rad	3.81%	8.40%	> 8.85%	19%
14	366 kN	1,184 kN-m	0.96	800 kN-m/% rad	2.47%	4.10%	None	55%
15	314 kN	1,072 kN-m	1.03	800 kN-m/% rad	5.45%	7.43%	8.94%	28%
16	316 kN	1,048 kN-m	1.03	750 kN-m/% rad	5.40%	6.36%	9.23%	24%

Specimen 14 was identical to Specimen 13, but it was loaded with 4,000 kN axial load as compared with 2,000 kN for Specimen 13. Specimen 14 exhibited a higher elastic stiffness and peak flexural resistance but has larger and more rapid degradation of resistance (55% loss) compared with Specimen 13. This is consistent with observations in prior research illustrated in Fig. 2. The hysteresis loops remain quite full with less pinching than any other specimen tested, and energy dissipation is quite large. However, the P- Δ moments reduce the lateral resistance of the connection, and these P- Δ moments exceed the connection resistant at approximately 7% connection rotation. The test was terminated shortly after this deformation to protect the testing equipment, because the actuator was supporting rather than loading the specimen. Dowel bar fracture did not occur for this test.

Specimens 15 and 16 used annular 19mm thick CDP and a 13mm thick ROFP, respectively, to improve constructability and to increase the stiffness of the connection. These two tests evaluated different pad thickness and material, since ROFP is a recycled material and less expensive than CDP. Comparing both tests with other specimens evaluates the effectiveness of the annular bearing pad concept. Both specimens experienced higher elastic and axial stiffness values than Specimen 13, and a slightly higher peak moment resistance. Spalling of the connection initiated at 5.5% connection rotation, a delay of 4.1% rotation and 1.7% rotation from Specimens 9 and 13 respectively. While the connection performance was

dramatically improved prior to initial spalling, Specimens 15 and 16 showed rapid loss of resistance after initiation of spalling. Nevertheless, the total deterioration was significantly smaller than that noted with Specimens 9, 10, and 14. Most spalling occurred as a single action for Specimens 15 and 16 rather than a continuous progression noted for other specimens. The spalling and deterioration of resistance at ultimate deformation were less severe for Specimens 15 and 16 than for other specimens, and there was not a dramatic difference in the CDP and ROFP performance. Specimens 15 and 16 also exhibited a delay in the initiation of dowel bar fracture.

The maximum moment resistance of all specimens was essentially identical for specimens with the bearing pads (Specimens 13, 14, 15 and 16) and for the current connection design (Specimen 9). At first glance, Table 2 suggests that the current design is 16% stronger than the modified bearing pad designs, but Table 1 shows that the yield stress of the dowel bars for Specimens 9 and 10 is 11% larger than that for Specimens 13 through 16. Since the flexural resistance of reinforced concrete is dominated by the yield stress, area, and placement of the reinforcing steel, the effective moment resistance for all specimens is nearly identical, as seen by comparing the normalized moment resistance as provided in Table 2.

There are distinct differences in performance for specimens with no bearing pad over the head of the pile (Specimens 9,10), specimens with a full CDP over the head of the pile (Specimens 13,14) and specimens with an annular CDP or ROFP over the head of the pile (Specimens 15,16). Figure 11 shows the visible connection damage for Specimens 9, 13, and 15 at a rotation of 0.05 radians. Specimen 9 has substantial spalling to the deck and the pile exposing the spiral reinforcing of the pile with some spalling beginning to penetrate the core of the pile. This spalling is comparable to that illustrated in prior tests of similar specimens in Fig. 3c. Specimen 13 experienced only moderate spalling to the pile cover, with no exposure of any reinforcing steel. Additionally the deck concrete is completely intact. Finally Specimen 15 has only pile cracking with no spalling to either the pile or the deck concrete. The advantages of the bearing pad connections, and in particular the annular pad configuration, is clear in comparison to other connections.

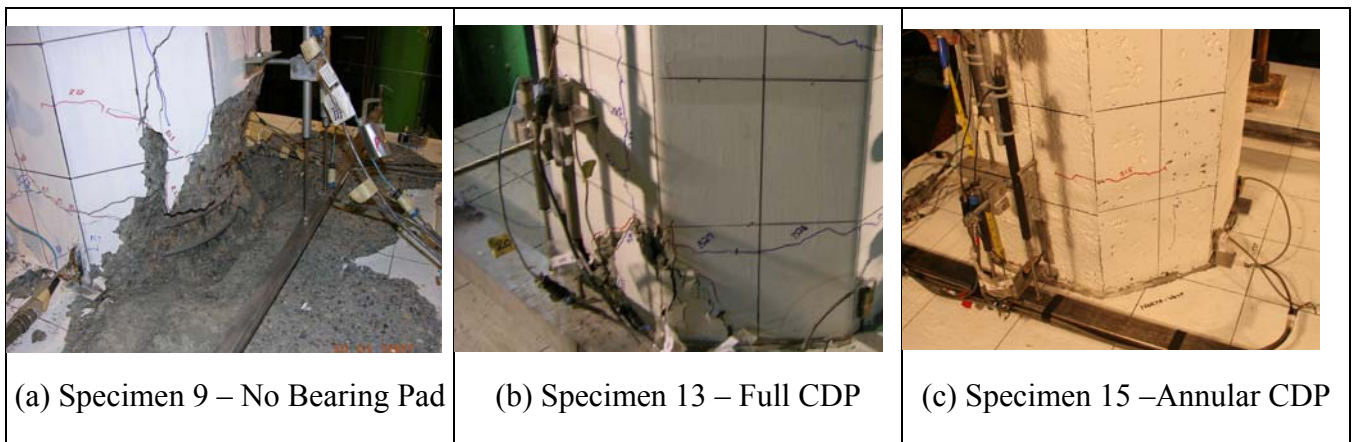


Figure 11. Visual Damage at Connection Rotation of 0.05 radians

Specimens 9, 10, 13, 14, 15, and 16 were evaluated in greater detail and their moment-rotation hysteretic response is shown in Fig. 9. The total connection moment includes the P- Δ effects caused by the axial loading on the pile. Therefore any observed strength loss in these plots can only be attributed to damage to the pile and connection. Specimens 11 and 12 are omitted from this detailed evaluation, because they were intermediary tests used to develop the damage resistant connection details. Table 2 details the performance of each specimen including peak shear and moment resistances, the normalized moment capacity (which compares the measured and predicted flexural strengths), the elastic rotational stiffness, the connection rotations at initial spalling, substantial spalling (exposure of reinforcing steel), and dowel bar fracture, as well as the deterioration in moment resistance at a connection rotation of 0.08 radians.

DESIGN PROCEDURE

The test results show that the specimens with debonded dowel bars, an annular CDP or ROFP over the head of the pile, and a flexible CFEM wrap around the embedded perimeter of the pile resulted in significant improvements in the seismic performance. A design procedure for this improved connection was developed from the accumulated research results. The design procedure focuses on the specific seismic detailing issues of the improved connection and does not address the analysis of the wharf deck, the pile body, or other general issues. The wharf layout, the size, detailing, and spacing of the piles must be designed to meet their respective performance objectives by usual design methods.

BEARING PAD THICKNESS

An annular CDP or ROFP placed over the head of the pile significantly improved the seismic performance over standard embedded dowel bar connections. The bearing pad should cover the head of the pile, with the circular hole having a diameter equal to the diameter of the outside perimeter of the dowel bar group as shown in Fig. 10.

While the depth of the compression block (or the location of the rotation point) varies depending on the end rotation of the pile, there is minimal fluctuation in the depth of the compression block at end rotations greater than 3% rotation (Stringer 2010). An appropriate approximate in the design is to assume a constant depth of 0.25D from the compressive face of the pile. The design thickness of the bearing pad is then selected using the design rotation and the maximum tolerable compressive strain in the bearing pad, as illustrated in Fig. 11. While testing of annular bearing pad connections is limited, the design recommendations for the bearing pad thickness use other bearing pad test results (Lehman et al. 2003, 2005).

Based upon geometry shown in Fig. 10, pad thickness, t_{pad} , can then be calculated using Equation 1.

$$t_{pad} = 0.25D \frac{\tan \theta}{\varepsilon_{p,CR}} \quad \text{Eq. (1)}$$

where, D is the pile diameter, θ_{spall} is the pile end rotation, and $\epsilon_{p,CR}$ is the critical strain limit for the bearing pad that results in spalling of the pile. Test results indicate $\epsilon_{p,CR}$ should be limited to 0.4 mm/mm for CDP and 0.6 mm/mm for ROFP. Equation 1 was used to develop the design plot presented in Figure 11, which gives the thickness of the bearing pad as a function of the pile diameter. The controlling pile end rotation was taken as 0.05 radians, because experiments show that at this rotation limit significant loss of resistance is prevented and significant repair is not required.

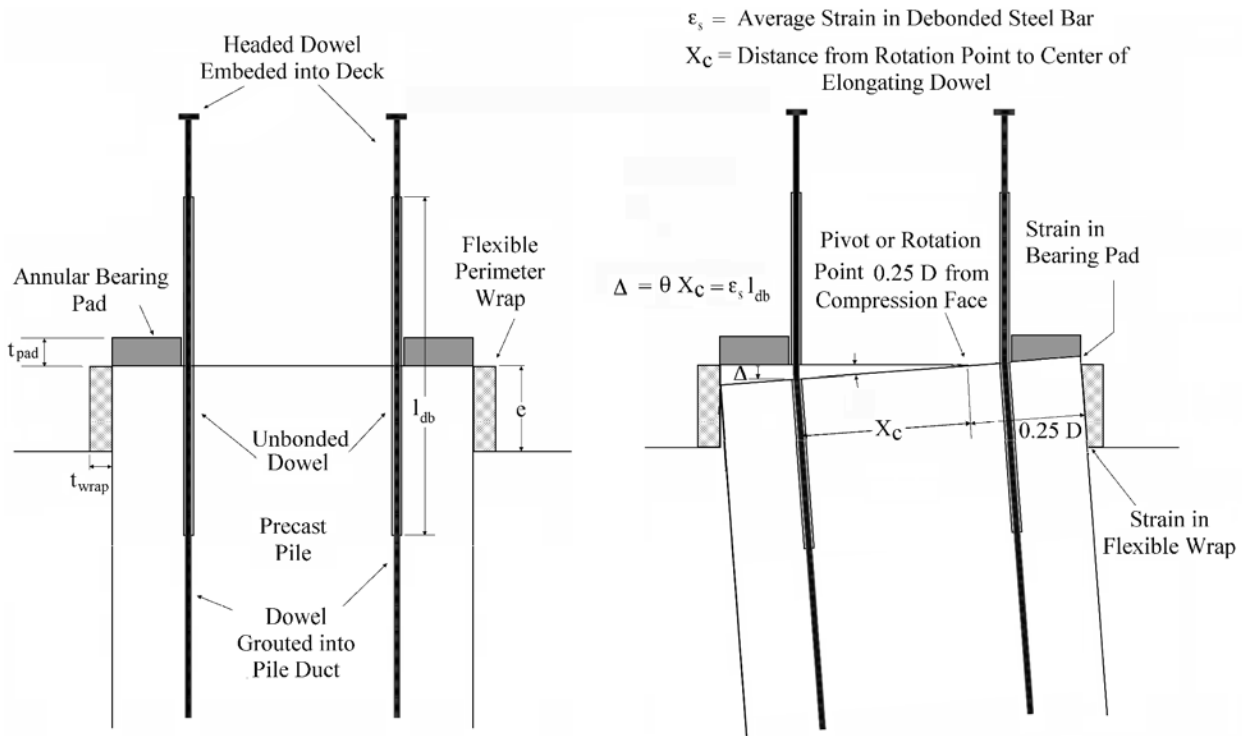


Figure 12. Geometry used to define bearing pad thickness

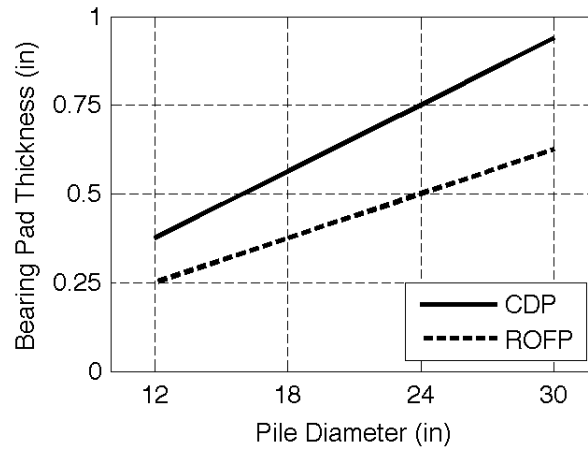


Figure 13. Bearing pad thickness design plot ($\theta_{spall} = 0.05$ radians)

CONNECTION STEEL

The connection between the pile and the deck is achieved with T-headed dowel bars grouted into ducts within the core of the pile. The dowel bars should be placed within the core of the pile, with the largest moment arm to make the connection as efficient as possible. With precast, prestressed concrete piles, the connection invariably has smaller moment resistance than the pile, because of the thick concrete cover required to protect the pile. The designer controls the number and size of the reinforcing bars and usually selects them to achieve the required connection moment capacity by ACI design methods (ACI 2008). In the case of a 610mm octagonal pile, the core typically has a radius of roughly 203mm, thus the dowels can be placed inside an 457mm circle, or centered on a 406mm inch circle when the width of the ducts, prestressing strands, and spiral reinforcing are taken into account.

DEBONDED LENGTH OF DOWEL BARS

Intentional debonding of the connection dowel bars reduces the strain concentrations in the steel and internal spalling of the concrete by distributing the strain along a longer length of the reinforcing bar. The design debonded length is determined based on the mechanics at the end of the pile illustrated in Fig. 12 and provided in Equation 2.

$$l_{db} = \theta_{fail} \frac{X_c}{\epsilon_{s,lim}} \quad \text{Eq. (2)}$$

Where θ_{fail} is the limiting connection rotation at connection failure as determined by dowel bar fracture, per performance objectives (taken as 0.085 radians), ϵ_{lim} is steel strain limit of 0.08 mm/mm, which correspond to a steel strain limit for A 706 steel bars subjected to multiple cyclic inelastic deformation cycles (Hawileh et al. 2010), and X_c is the distance from the point of rotation to the extreme tension bar.

INTERFACE SHEAR RESISTANCE

Design engineers frequently employ direct bearing between the side of the embedded length of the pile and the deck soffit cover concrete to develop shear transfer between the pile and deck superstructure in current practice. With current embedded dowel connections, experimental results show that this bearing is lost at relatively small deformations. With the improved connection, a flexible joint material is wrapped around the perimeter of the embedded length of the pile, as a result, shear resistance at the interface is developed by the shear sliding resistance only. Experimental results show that in annular bearing pad connections the bearing pad experiences less than 0.01 mm/mm axial strain under 2000 kN axial load (10% gross axial capacity of the pile). CDP has a compressive stiffness of approximately 210 MPa (Lehman et al. 2003), which is two orders of magnitude more flexible than the concrete core, and so the annular bearing pad sustains a compressive stress of approximately 2 MPa. This indicates that the annular pad carries a very small portion of

the axial load. Therefore, the concrete core effectively resists the entire axial load on the connection.

The concrete core can be used to quantify the shear resistance of the connection through friction. This resistance is defined in Equation 3, which modifies the shear friction design procedure outlined in ACI Section 11.6 to account for the compressive stress on the interface (ACI 2008).

$$V_{sf} = \mu(P + f_y A_{vf}) \quad \text{Eq. (3)}$$

Where, μ is the coefficient of friction as defined by ACI 318 Section 11.6.4.3 according to the surfaces in contact (which may be approximated as 0.6 for concrete cast against hardened but not intentionally roughened concrete), P is the axial load on the connection, A_{vf} is the area of reinforcing steel crossing perpendicular to the shear plane, and f_y is the yield strength of the reinforcing steel resisting shear sliding. ACI stipulates that the shear resistance due to shear friction as calculated by Eq. 3 cannot exceed the lesser of the following limits:

$$V_{sf,max} = \min \left\{ \begin{array}{l} 0.2 f'_c A_{core} \\ 5.5 A_{core} (MPa) \end{array} \right. \quad \text{Eq. (4)}$$

The total shear resistance therefore is taken as the sum of the resistances due to the bearing pad and concrete core shear friction.

$$V_n = V_{sf} + V_{bp} \quad \text{Eq. (5)}$$

Finally the factored shear resistance (ϕV_n) must be greater than the applied shear on the connection (V_u).

$$V_u \leq \phi V_n \quad \text{Eq. (6)}$$

This shear friction alone is conservative; it neglects all bearing capacity through the flexible joint sealant used to wrap the embedded pile, and the friction and shear resistance of the annular pad caused the large compressive stress due to the bending moment associated with the pile shear force. However, this shear capacity alone should be adequate for most applications. For example the 2000 kN compressive force used in these experiments, the shear capacity ϕV_n was 685 kN, while the maximum demand associated with the maximum bending capacity of the connection was 356 kN. If additional, shear resistance is required, the shear resistance of friction between the concrete deck and bearing pad can be included. In that case, the additional strength would be:

$$V_{bp} = \mu_{bp} * C_c \quad \text{Eq. (7)}$$

where μ_{bp} is the coefficient of friction can be conservatively taken as 0.2 (Lehman et al. 2005) and C_c is the compressive force of the moment couple.

FLEXIBLE JOINT SEALANT WRAP THICKNESS

The CFEM flexible joint sealant wrapped around the perimeter of the embedded pile section of seals the joint interface and permits large connection rotations without spalling of the pile and deck or the resulting deterioration in resistance. The wrap must be thick enough to prevent the side of the pile coming in contact with the deck soffit cover concrete, so that at the maximum expected rotation of the pile end the edge of the pile should avoid contact with the deck cover concrete as depicted in Fig. 9.

The design equation is generated from the geometric relationship shown in Eq. 8, and strain in the CFEM is limited to 0.5 mm/mm.

$$t_{wrap} = 2(t_{pad} + e) \tan(\theta_{fail}) \quad \text{Eq. (8)}$$

Where t_{pad} is the nominal thickness of the bearing pad, e is the embedment depth of the pile into the deck soffit cover concrete, and θ_{fail} is the maximum rotation expected within the connection (taken as 0.085 rad.) as determined by performance objectives. The CFEM expansion material is recommended, and it has a secant stiffness of between 70 kPa and 170 kPa at 25% compressive strain.

CONCLUSIONS AND RECOMMENDATIONS

This research has evaluated embedded dowel moment resisting prestressed concrete pile-to-wharf connections that are commonly used in current seismic design of marginal wharves and developed an improved connection that significantly delays the damage and deterioration of moment resistance of the pile, wharf deck and connection until much larger seismic deformations.

When combined with prior research, this study shows that current connections sustain significant damage and deterioration of resistance starting at relatively small seismic deformations. In particular they:

- Have early onset of pile and deck spalling at relatively small inelastic deformations. Significant spalling to the deck soffit cover concrete, and severe spalling into the core of the pile was noted with increasing deformation. This spalling causes dramatic loss in resistance even at moderate deformation levels. The spalling damage and resulting deterioration of resistance that results from this damage increases dramatically with increasing compressive axial load.
- The spalling damage requires significant repair even after moderate seismic deformation levels.
- Extended pile connections that are used when the pile driven below the bottom level of the wharf deck, exhibit different behavior, which is closer to that of cast-in-place reinforced concrete moment connection.

As a consequence of this behavior, research was completed to develop an improved connection for the prestressed concrete piles. The research showed that:

- The addition of a bearing pad over the head of the pile reduces the initial elastic stiffness of the connection compared to current connection designs. It significantly delays (by approximately 0.04 radian connection rotation compared to standard connections) pile and connection damage, yet achieves the same maximum resistance and inelastic deformation capacity as the current connection. The post-peak strength degradation is reduced.
- The addition of a CFEM flexible joint sealant wrapped around the perimeter of the embedded pile segment effectively eliminates spalling of the wharf deck.
- Connections employing a full CDP over the head of the pile displaced in near rigid body rotation with on average 90% of the pile tip displacement resulting from end rotation of the pile at the interface. They also experienced axial deformations due to the low compressive stiffness of the pad material.
- Annular bearing pad connections also experienced mostly rigid body rotation but to a slightly lesser degree than the full pad connections, with approximately 80% of the measured displacement resulting from end rotation of the pile. These specimens have a higher elastic lateral stiffness than full bearing pad connections, and they maintained similar axial stiffness noted with current connection design due to the concrete plug in the center of the annular bearing pad.
- The normalized moment resistance of the connections subjected the same axial load were similar and symmetric.
- Higher axial load resulted in larger moment resistance, greater deterioration of resistance and greater loss of effective resistance due to P- Δ effects.
- Spalling of the pile cover concrete coincides with bearing pad strains of 0.4 and 0.6 mm/mm for CDP and ROFP materials, respectively.

An improved moment resisting connection is proposed and significant improvements in performance are achieved. This connection:

- Employs a CDP or ROFP bearing pad over the head of the pile. The pad is an octagonal shaped annular ring, which covers all the pile concrete outside the perimeter of dowel bars. The annular ring permits easier placement of the grouted dowel bars, and it improves the stiffness and deformation of the connection. The improved connection also includes a flexible CFEM wrap around the perimeter of the embedded section of the pile, and the dowel bars are deliberately debonded over a significant length.
- These changes results in 1) significant delays and reductions in spalling of the pile and wharf deck, 2) identical maximum moment resistance of the connection, 3) large reductions in the deterioration of resistance of the connection, 4) large reductions in repairs required after seismic deformation with no repair required for connection rotations in the order of 0.05 radians, and 5) slightly larger total rotational capacity than the current connection design.
- A design procedure for the improved connection is developed and presented.

Due to limitations in time and funding of this research, several areas were not addressed and warrant further study. These include:

- The annular bearing pad connections were only tested under one level of axial load (10% gross axial capacity of the pile), thus it would be prudent to examine the behavior of the connection under higher (20% axial capacity) and lower (5% axial capacity) axial loads.
- Full bearing pad connections should be tested using different pad thicknesses and materials.

ACKNOWLEDGEMENTS

This work was funded primarily by the National Science Foundation as part of a NEESR Grand Challenge "Seismic Risk Management for Port Systems" grant to Georgia Institute of Technology. This work was completed under subagreement E-20-L05-G3 between the University of Washington and Georgia Institute of Technology. Prof. Glenn Rix is the principle investigator of the grand challenge research. Additional financial support was provided by the Pacific Engineering Research Center through agreement FA40186/A44763 with Prof. Stephen Mahin coordinating the program. The piles were all generously donated by Concrete Technology Corporation, facilitated by Steven Seguirant. Financial support for graduate students was provided by the firm of Moffat and Nichol and the Prestressed Concrete Institute. This financial support is gratefully acknowledged. The authors express special thanks to Stu Werner, Michael Jordan, George Fotinos, Erik Soderberg and Robert Harn for their technical advice and guidance.

BIBLIOGRAPHY

1. ACI (2008). *ACI 318-08 Building Code Requirements for Structural Concrete and Commentary*. American Concrete Institute, 2008.
2. ATC, (1992). "ATC-24 Guidelines for Testing Steel Components," Applied Technology Council, Redwood City CA, 57 pp.
3. Bell, J.K., (2008). *Seismic Testing of Existing Full Scale Pile to Deck Connections: Precast Prestressed and Steel Piles*. Masters Thesis, University of California, San Diego.
4. Chang, S.E., (2000) "Disasters and Transport Systems: Loss, Recovery and Competition at the Port of Kobe after the 1995 Earthquake." *Journal of Transport Geography*, Aug 2000: 53-65.
5. Graff, R., (2001). *Seismic Evaluation of Prestressed Pile-Wharf Connections*. Masters Thesis, University of Washington, Seattle.
6. Harn, R., Mays, T.W., and Johnson, G.S., (2010). "Proposed Seismic Detailing Criteria for Piers and Wharves." *Ports 2010*. ASCE. 460-469.
7. Hawileh, R., Rahman, A. and Tabatabai, H. (2010) "Evaluation of the Low-Cycle Fatigue Life in ASTM A706 and A615 Grade 60 Steel Reinforcing Bars" *ASCE Journal of Materials in Civil Engineering*, Vol. 22, No. 1, January 1, 2010.
8. Jellin, A.R., (2008). *Improved Seismic Connections for Pile-Wharf Construction*. Masters Thesis, University of Washington, Seattle.
9. Joen, P.H., and Park, R. (1990). "Simulated Seismic Load Tests on Prestressed Piles and Pile-Pile Cap Connections." *PCI Journal*, Nov-Dec: 42-61.
10. Krier, C.J. (2006). *Seismic Testing of Full Scale Precast Prestressed Pile to Deck Connections*. Masters Thesis, University of California, San Diego.
11. Lehman, D.E., Roeder, C.W., and Larsen, R.E., (2005) "Design of Cotton Duck Bridge Bearing Pads," ASCE, *Journal of Bridge Engineering*, Vol. 10, No.5, September, pgs 555-63.
12. Lehman, D.E., Roeder, C.W., Larsen, R., and Curtin, K., (2003). *Cotton Duck Bearing Pads: Engineering Evaluation and Design Recommendations*. Research Report, Washington State Department of Transportation.
13. Matsumoto, E.E., Waggoner, M.C., Kreger, M.E., Vogel, J., and Wolf, L., (2008) . "Development of a Precast Concrete Bent-Cap System." *PCI Journal* (PCI), May-June 2008: 74-99.
14. Meadows (2001). "Specification for CERAMAR Sealtight Flexible Foam Expansion Joint, W.R. Meadows Company, Hampshire, IL.
15. MOTEMS (2005). "Marine Oil Terminals," California Building Code, Chapter 31F (For SLC).
16. Pizzano, B.A. (1984). *Behavior of Prestressed Concrete Piles Under Seismic Loading*. Masters Thesis, University of Washington, Seattle.
17. Port of Seattle, (2009). "Foreign Waterborne Trade Report," Port of Seattle, Seattle, WA.

18. Roeder, C.W., Graff, R., Soderstrom, J., and Yoo, J-H, (2005). "Seismic Performance of Pile-Wharf Connections." *Journal of Structural Engineering* (ASCE), March 2005: 428-437.
19. Silva, P.F. (1998) *Experimental and Analytical Models to Predict the Response of Pile to Pile Cap Connections Under Simulated Seismic Loads*. Doctoral Dissertation, University of California, San Diego.
20. Silva, P., Seible, F., Priestley, N., (1997) *Response of Standard CALTRANS Pile-to-Pile Cap Connections Under Simulated Loads*. Report No. SSRP-97/09, UC San Diego: Division of Structural Engineering.
21. Soderstrom, J., (2001). *Seismic Evaluation of Prestressed and Reinforced Concrete Pile-Wharf Deck Connections*. Masters Thesis, University of Washington, Seattle, 2001.
22. Sritharan, S, and Priestley, N. (1998). *Seismic Testing of a Full-Scale Pile-Deck Connection Utilizing Headed Reinforcement*. Report, University of California, San Diego.
23. Stanton, J.F., Stone, W.C. and Cheok, G.S. (1997). "A Hybrid Reinforced Precast Frame for Seismic Regions". *PCI Jo.* 42(4), March-April, 20-33.
24. Steuck, K.P., Pang, J.B.K., Eberhard, M.O., and Stanton, J.F., (2007). *Anchorage of Large Diameter Reinforcing Bars Grouted Into Ducts*. Research Report, Washington State Transportation Center.
25. Stringer, S.J. (2010). *Seismic Performance of Improved Damage Resistant Pile to Wharf Deck Connections*. Masters Thesis, University of Washington, Seattle, 2010.
26. Yoo, J-H. (2001) *Dynamic Analysis of Pile-to-Wharf Connections*. Masters Thesis, University of Washington, Seattle.